Growth and properties of GaSbBi alloys

M. K. Rajpalke,[1,a)] W. M. Linhart,[1,a)] M. Birkett,[1] K. M. Yu,[2] D. O. Scanlon,[3,4] J. Buckeridge,[4] T. S. Jones,[5] M. J. Ashwin,[5,b)] and T. D. Veal[1,c)]
[1]*Stephenson Institute for Renewable Energy and Department of Physics, School of Physical Sciences, University of Liverpool, Liverpool L69 7ZF, United Kingdom*
[2]*Materials Sciences Division, Lawrence Berkeley National Laboratory, 1 Cyclotron Road, Berkeley, California 94720, USA*
[3]*Diamond Light Source Ltd., Diamond House, Harwell Science and Innovation Campus, Didcot, Oxfordshire OX11 0DE, United Kingdom*
[4]*Kathleen Lonsdale Materials Chemistry, Department of Chemistry, University College London, 20 Gordon Street, London WC1H 0AJ, United Kingdom*
[5]*Department of Chemistry, University of Warwick, Coventry CV4 7AL, United Kingdom*

(Received 25 July 2013; accepted 18 September 2013; published online 2 October 2013)

Molecular-beam epitaxy has been used to grow $GaSb_{1-x}Bi_x$ alloys with x up to 0.05. The Bi content, lattice expansion, and film thickness were determined by Rutherford backscattering and x-ray diffraction, which also indicate high crystallinity and that >98% of the Bi atoms are substitutional. The observed Bi-induced lattice dilation is consistent with density functional theory calculations. Optical absorption measurements and valence band anticrossing modeling indicate that the room temperature band gap varies from 720 meV for GaSb to 540 meV for $GaSb_{0.95}Bi_{0.05}$, corresponding to a reduction of 36 meV/%Bi or 210 meV per 0.01 Å change in lattice constant. © *2013 AIP Publishing LLC*. [http://dx.doi.org/10.1063/1.4824077]

Additional flexibility in III–V semiconductor band gap and lattice constant engineering has been achieved in the last two decades by exploiting band anticrossing interactions in so-called highly mismatched alloys.[1] These include dilute nitrides, and increasingly, dilute bismides, where there is a mismatch between the size and electronegativity of the host anions and the isoelectronic impurity element. Here the focus is upon GaSb based highly mismatched alloys which are of interest for 2–5 μm midinfrared applications. While tuning of the band gap within this range has recently been achieved using GaN_xSb_{1-x} alloys,[2,3] changing the band gap of GaSb by Bi alloying has yet to be adequately explored. This is in spite of the fact that the closely related InSbBi alloy system was the first of the dilute bismide materials to be grown,[4–6] long before the band anticrossing phenomena became established.[7] The previous recent reports of the growth of $GaSb_{1-x}Bi_x$ alloys by liquid-phase and molecular-beam epitaxy (MBE) were characterized by low levels of Bi incorporation with $x \leq 0.008$ (Refs. 8 and 9) and lattice contraction with respect to GaSb rather than the expected expansion.[9]

This letter reports the growth by molecular-beam epitaxy of GaSbBi alloys with up to 5% Bi, characterization by x-ray diffraction (XRD), Rutherford backscattering (RBS) and optical absorption spectroscopy, and density functional theory (DFT) calculations of Bi substitution into GaSb.

The GaSbBi epilayers for this study were grown by solid source MBE on GaSb (001) undoped substrates mounted on In-free platens. Each of the substrates was outgassed at 300 °C prior to loading into the growth chamber. The Ga flux was supplied by a Sumo cell, the Sb flux by an Addon valved cell, and the Bi flux by a downward facing Sumo cell. For each substrate, the oxide was removed under an incident Sb flux at approximately 550 °C and then a 100 nm GaSb buffer layer was grown at 500 °C. Thereafter, the substrate was cooled to the required temperature under an Sb flux, with the incident Sb being removed when the substrate temperature reached 370 °C. The Bi beam equivalent pressure flux was then set to approximately 3.3×10^{-8} millibars using the beam monitoring ion gauge. Once the cells had settled at the desired values, a ~320 nm-thick GaSbBi epilayer was grown. The samples were grown at a fixed growth rate of ~0.4 μmh^{-1} but over a range of substrate temperatures (250–350 °C). Growth temperatures were determined using a pyrometer.

The samples were examined *ex situ* using RBS with 3.72 MeV He^{2+} ions, an Asylum atomic force microscope (AFM), and by high-resolution XRD using a Philips X'Pert diffractometer equipped with a monochromatic Cu K_α x-ray source ($\lambda = 0.15406$ nm) and a four bounce Ge monochromator. Analysis of the XRD measurements of the 004 reflections was performed using the X'pert Epitaxy application. Transmittance measurements were performed at room temperature using a Bruker Vertex 70 V Fourier-transform infrared spectrometer, using a liquid nitrogen-cooled HgCdTe detector, KBr beam splitter, and a globar light source. The absorption coefficient, α, was calculated from the transmittance data using Eq. (2) in Ref. 10.

Due to the lack of an experimentally determined zinc blende GaBi lattice parameter precluding composition determination from XRD, the Bi fraction in the GaSbBi films and their thickness was determined by RBS. The inset of Fig. 1 shows the RBS spectrum from the sample grown at 250 °C, along with simulated contributions from Bi, Sb, and Ga atoms, using the SIMNRA code,[11] indicating a $GaSb_{1-x}Bi_x$ composition corresponding to Bi occupying 5% of the anion sublattice or $x = 0.05$. The step in the Sb signal at ~3.1 MeV corresponds to the change from 95% Sb occupation of the

[a)]M. K. Rajpalke and W. M. Linhart contributed equally to this work.
[b)]Electronic mail: M.J.Ashwin@warwick.ac.uk
[c)]Electronic mail: T.Veal@liverpool.ac.uk

anion sublattice in the GaSbBi film to 100% Sb in the GaSb buffer layer and substrate. This indicates that the Bi incorporates on the group V sublattice. The Bi content from RBS as a function of growth temperature is shown in Fig. 1 for fixed Bi cell conditions and fixed growth rate. The Bi content increases as the growth temperature decreases and reaches a plateau corresponding to $x = 0.05$ for growth temperatures below approximately 275 °C. The temperature dependence of the Bi incorporation in $GaSb_{1-x}Bi_x$ has been modeled using the kinetic approach described by Wood *et al.*[12] and Pan *et al.*[13] that has previously been applied to N incorporation in $Ga(In)N_xSb_{1-x}$ alloys.[3,14] The curve shown in Fig. 1 corresponds to an energy barrier for Bi desorption of 1.75 eV and a characteristic surface residence lifetime of Bi atoms of 6.5 μs, compared with the previously reported values for GaNSb of 2.0 eV for the barrier for N desorption and 5 μs for the characteristic surface residence lifetime of N atoms.[14] Channeling RBS measurements along the ⟨100⟩, ⟨110⟩, and ⟨111⟩ directions indicate that the films have very high epitaxial quality with greater than 98% of the Bi atoms in the substitutional group V sublattice in all films.

AFM measurements have previously indicated that large Bi droplets can form on the surface of GaSbBi grown with high Bi flux, but flat surfaces with root mean squared (RMS) roughnesses below 1 nm have been obtained using lower Bi fluxes.[9] Here, a 2.5 × 2.5 μm^2 atomic force micrograph of the sample grown at 300 °C indicates a similar RMS roughness of 0.65 nm.

XRD was used to determine the epitaxial quality of the films and to confirm the epilayer thickness. An example measurement and simulation is shown in Fig. 2 for a layer with $x = 0.036$, where both the 004 peak splitting and the Pendellösung fringes were modeled by dynamical simulations. The epilayer peak occurs at lower Bragg angle than the substrate peak, corresponding to the GaSbBi layer having an expanded lattice with respect to that of GaSb. This lattice dilation is in contrast to the aforementioned lattice contraction of GaSbBi observed by Song *et al.*[9]

The tetragonal distortion of the pseudomorphic GaSbBi films is accounted for using GaSb elastic constants. There is

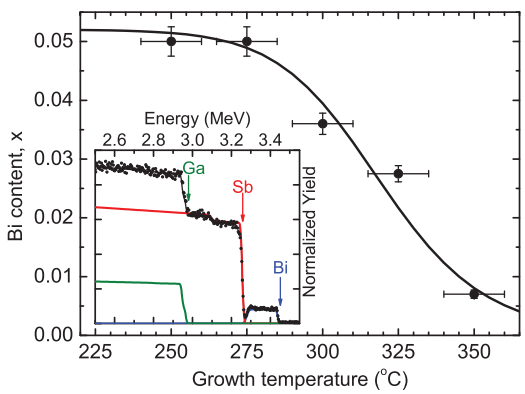

FIG. 1. The Bi content measured by RBS in $GaSb_{1-x}Bi_x$ films as a function of growth temperature at a fixed growth rate of 0.4 μmh^{-1} and fixed Bi flux. The points are the experimental data. The solid line is the calculated dependence from kinetic modeling. The inset contains the RBS data (points) from a film grown at 250 °C with $x = 0.05$. The blue, red, green, and black lines correspond to the Bi, Sb, Ga, and total simulated contributions to the spectrum.

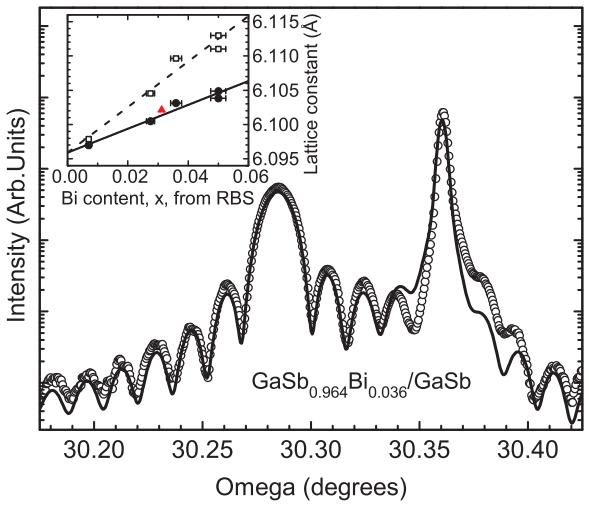

FIG. 2. XRD (points) of the 004 diffraction maximum from a GaSbBi film grown on a GaSb substrate at 300 °C at a growth rate of 0.4 $\mu m\ h^{-1}$. The simulation (solid line) indicates that the GaSbBi film thickness is 310 ± 10 nm. The inset shows the lattice parameters measured by XRD in the growth direction of the pseudomorphic GaSbBi films (open squares) as a function of the Bi content from RBS and the derived lattice parameters for free standing GaSbBi (closed circles). The dashed and solid lines are linear fits, respectively, to the measured and derived lattice parameter data, constraining the $x = 0$ intercept to be at 6.0959 Å, the lattice parameter of GaSb.

good agreement between the experimental and simulated XRD patterns. All samples show clear thickness fringes, indicating the presence of smooth and coherent interfaces. The lattice parameters in the growth direction of the pseudomorphic films are shown in the inset of Fig. 2 as a function of RBS-determined Bi content (open squares), along with the corresponding derived free standing GaSbBi lattice parameters (closed circles). The lattice parameter varies linearly, following Vegard's law.

The incorporation of Bi in GaSb has also been investigated using DFT calculations employing hybrid functionals which often provide better structural data and more accurate band gaps than the local density and generalized gradient approximations.[15–17] Here, the screened Heyd-Scuseria-Ernzerhof (HSE) hybrid density functional is used,[18] as implemented in the VASP code.[19] The value of exact nonlocal exchange, α, was 32.5%, which yields a band gap of 841 meV for GaSb, in good agreement with the 0 K band gap of 812 meV extrapolated from low temperature experimental data.[20] The valence–core interaction was described using the projector augmented wave (PAW) approach,[21] and cores of [Ar] for gallium, [Kr] for antimony, and [Xe] for bismuth are used. A cutoff of 400 eV was used for all the calculations, with the Brillouin zone sampled using a 8 × 8 × 8 Monkhorst Pack grid. Calculations were deemed to have converged when the forces on all the atoms were less than 0.01 eV $Å^{-1}$, and all calculations included spin-orbit-coupling.

To assess the formation energy of Bi alloying with GaSb, we have calculated the formation energy for substitution of Bi on the anion sublattice, Bi_{Sb}, and for Bi substitution on the cation sublattice, Bi_{Ga}. Supercells containing 64 atoms were created, in which 1 Bi atom corresponds to $x = 0.03125$ in $GaSb_{1-x}Bi_x$. A k-point mesh of Γ-centered 2 × 2 × 2 was used for the supercell calculations, and the impurity formation

energies are calculated using the standard approach.[22] The formation energy for Bi_{Sb} is 0.59 eV under Sb-rich and 0.22 eV for Sb-poor conditions, while Bi_{Ga} is 1.75 eV for Sb-rich and 2.33 eV for Sb-poor conditions. This indicates that substitution of Bi on the anion sublattice is very likely, in agreement with our experimental results, and that significant concentrations of cation substitution by Bi is highly unlikely. The inclusion of one Bi_{Ga} defect in a 64 atom supercell gives a 1.54% volume expansion, compared with 0.35% volume expansion for Bi_{Sb}. This corresponds to a 0.117% linear expansion for Bi on the Sb site for a $GaSb_{1-x}Bi_x$ alloy composition corresponding to $x = 0.03125$. Applying this expansion to the room temperature, experimental GaSb lattice parameter gives the triangle data point in the inset of Fig. 2, which is in agreement with the experimentally determined lattice expansion resulting from Bi alloying.

In order to investigate the optical properties of the GaSbBi samples as a function of Bi content, transmittance measurements were performed. The transmission data from each sample was divided by the transmission from a GaSb substrate so that the remaining signal corresponds to transmission through a ~320-nm thick GaSbBi layer. The derived absorption spectra are shown in Fig. 3. The absorption edge decreases in energy to ~540 meV as the Bi content is increased to $x = 0.05$. The observed decrease exceeds the band gap reduction predicted by the virtual crystal approximation (VCA) (that is, linear variation of the band gap between the two zinc-blende binary end points of the alloy). Using the hybrid DFT-calculated "negative band gap" of the semi-metallic zinc-blende GaBi of −2.14 eV (Ref. 23), the VCA band gap reduction, shown by the dashed line in Fig. 3, is 26.3 meV/%Bi consisting of 26.0 meV/%Bi lowering of the conduction band minimum (CBM) and 0.3 meV/%Bi increase of the valence band maximum (VBM). However, the band gap reduction is well reproduced by the $12 \times 12\,\mathbf{k}\cdot\mathbf{p}$ model described by Alberi *et al*. for GaAsSb and GaAsBi[24] wherein a valence band anticrossing (VBAC) interaction is included between localized Bi 6 *p*-like states and the host valence bands. Here, the Bi state energy level is 1.17 eV below the GaSb VBM and the interaction strength is 1.1 eV. The VBAC interaction is combined with the effect of lowering of the CBM within the VCA.

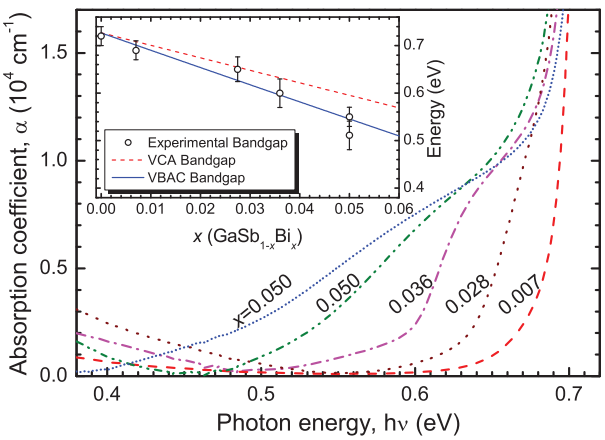

FIG. 3. The absorption spectra for $GaSb_{1-x}Bi_x$ films grown at different temperatures. The composition of each film is given in the figure. The inset shows the band gap versus Bi content determined from the absorption spectra. The dashed line is the band gap of $GaSb_{1-x}Bi_x$ calculated assuming the VCA variation of both the CBM and the VBM and the solid line is the band gap of $GaSb_{1-x}Bi_x$ calculated assuming the VCA variation of the CBM and VBAC between the valence bands and the Bi impurity level.

The band gap reduction is 36.2 meV/%Bi and, according to the modeling, is made up of 26.0 meV/%Bi VCA lowering of the CBM and 10.2 meV/%Bi due to the upward shift of the VBM due to the VBAC interaction. This total band gap reduction of 36 meV/Bi% is significantly lower than the ~84 meV/%Bi for GaAsBi.[25] The 10 meV/%Bi upward VBM shift for GaSbBi is much smaller than equivalent value for GaAsBi of 53 meV/%Bi.[26] This is consistent with the smaller size and electronegativity mismatch between Sb and Bi as compared to As and Bi. However, in terms of band gap reduction per unit of lattice constant change, GaSbBi is one of the most extreme highly mismatched alloys. Comparing the band gap reduction for 0.01 Å change of lattice constant, the value of 210 meV for GaSbBi exceeds those for GaNSb (105 meV),[2] GaNAs (157 meV) (Refs. 27 and 28), and GaAsBi (125 meV).[25] This is largely a consequence of the relatively close proximity of the GaSb and zinc-blende GaBi lattice parameters.

In summary, $GaSb_{1-x}Bi_x$ thin films with x up to 0.05 have been grown by MBE. The Bi was found to cause the expected expansion of the lattice, in contrast to some previous reports, and greater than 98% of the incorporated Bi was found to be substitutional on the Sb sublattice. This is consistent with our hybrid functional DFT results. The optical absorption edge was found to decrease from 720 meV for GaSb to ~540 meV for $GaSb_{0.95}Bi_{0.05}$. The band gap reduction corresponds to 36 meV/%Bi, much lower than the 84 meV/%Bi for GaAsBi, but in terms of the 210 meV band gap reduction per 0.01 Å change of lattice constant, GaSbBi is one of the most extreme highly mismatched alloys.

The work at Liverpool and Warwick was supported by the University of Liverpool and the Engineering and Physical Sciences Research Council (EPSRC) under Grant Nos. EP/G004447/2 and EP/H021388/1. RBS measurements performed at Lawrence Berkeley National Lab were supported by the Director, Office of Science, Office of Basic Energy Sciences, Materials Sciences and Engineering Division, of the U.S. Department of Energy under Contract No. DE-AC02-05CH11231. Calculations were performed on the IRIDIS cluster provided by the EPSRC-funded Centre for Innovation (EP/K000136/1 and EP/K000144/1), and the HECToR supercomputer via the UK's HPC Materials Chemistry Consortium (EP/F067496). DOS acknowledges the Ramsay Memorial Trust and UCL for a Ramsay Fellowship. DOS and TDV acknowledge membership of the Materials Design Network. Luke Rochford is gratefully acknowledged for performing the AFM measurements.

[1]W. Walukiewicz, K. Alberi, J. Wu, W. Shan, K. M. Yu, and J. W. Ager III, *Physics of Dilute III–V Nitride Semiconductors and Material Systems: Physics and Technology* (Springer, Berlin, 2008), Chap. 3.
[2]J. J. Mudd, N. J. Kybert, W. M. Linhart, L. Buckle, T. Ashley, P. D. C. King, T. S. Jones, M. J. Ashwin, and T. D. Veal, Appl. Phys. Lett. **103**, 042110 (2013).
[3]M. J. Ashwin, D. Walker, P. A. Thomas, T. S. Jones, and T. D. Veal, J. Appl. Phys. **113**, 033502 (2013).

[4]B. Joukoff and A. M. Jean-Louis, J. Cryst. Growth **12**, 169 (1972).
[5]J. L. Zilko and J. E. Greene, Appl. Phys. Lett. **33**, 254 (1978).
[6]K. Oe, S. Ando, and K. Sugiyama, Jpn. J. Appl. Phys., Part 2 **20**, L303 (1981).
[7]W. Shan, W. Walukiewicz, J. W. Ager, E. E. Haller, J. F. Geisz, D. J. Friedman, J. M. Olson, and S. R. Kurtz, Phys. Rev. Lett. **82**, 1221 (1999).
[8]S. K. Das, T. D. Das, S. Dhar, M. de la Mare, and A. Krier, Infrared Phys. Technol. **55**, 156 (2012).
[9]Y. Song, S. Wang, I. S. Roy, P. Shi, and A. Hallen, J. Vac. Sci. Technol. B **30**, 02B114 (2012).
[10]C. Ghezzi, R. Magnanini, A. Parisini, B. Rotelli, L. Tarricone, A. Bosacchi, and S. Franchi, Phys. Rev. B **52**, 1463 (1995).
[11]L. Mayer, "SIMNRA, a simulation program for the analysis of NRA, RBS, and ERDA," in *Proceedings of the 15th International Conference on Application Accelerators in Research and Industry*, edited by J. L. Duggan and I. L. Morgan (AIP, NY, 1999), Vol. 475, p. 541.
[12]C. E. C. Wood, D. Desimone, K. Singer, and G. W. Wicks, J. Appl. Phys. **53**, 4230 (1982).
[13]Z. Pan, L. H. Li, W. Zhang, Y. W. Lin, and R. H. Wu, Appl. Phys. Lett. **77**, 214 (2000).
[14]M. J. Ashwin, T. D. Veal, J. J. Bomphrey, I. R. Dunn, D. Walker, P. A. Thomas, and T. S. Jones, AIP Adv. **1**, 032159 (2011).
[15]M. Burbano, D. O. Scanlon, and G. W. Watson, J. Am. Chem. Soc. **133**, 15065 (2011).
[16]D. O. Scanlon, A. B. Kehoe, G. W. Watson, M. O. Jones, W. I. F. David, D. J. Payne, R. G. Egdell, P. P. Edwards, and A. Walsh, Phys. Rev. Lett. **107**, 246402 (2011).
[17]J. P. Allen, D. O. Scanlon, and G. W. Watson, Phys. Rev. B **81**, 161103(R) (2010).
[18]A. V. Krukau, O. A. Vydrov, A. F. Izmaylov, and G. E. Scuseria, J. Chem. Phys. **125**, 224106 (2006).
[19]G. Kresse and J. Furthmüller, Phys. Rev. B **54**, 11169 (1996).
[20]I. Vurgaftman and J. R. Meyer, J. Appl. Phys. **94**, 3675 (2003).
[21]P. E. Blöchl, Phys. Rev. B **50**, 17953 (1994).
[22]D. O. Scanlon, P. D. C. King, R. P. Singh, A. de la Torre, S. McKeown Walker, G. Balakrishnan, F. Baumberger, and C. R. A. Catlow, Adv. Mater. **24**, 2154 (2012).
[23]D. O. Scanlon and J. Buckeridge (unpublished).
[24]K. Alberi, J. Wu, W. Walukiewicz, K. M. Yu, O. D. Dubon, S. P. Watkins, C. X. Wang, X. Liu, Y.-J. Cho, and J. Furdyna, Phys. Rev. B **75**, 045203 (2007).
[25]S. Tixier, M. Adamcyk, T. Tiedje, S. Francoeur, A. Mascarenhas, P. Wei, and F. Schiettekatte, Appl. Phys. Lett. **82**, 2245 (2003).
[26]C. A. Broderick, M. Usman, S. J. Sweeney, and E. P. O'Reilly, Semicond. Sci. Technol. **27**, 094011 (2012).
[27]M. Weyers, M. Sato, and H. Ando, Jpn. J. Appl. Phys., Part 2 **31**, L853 (1992).
[28]K. Uesugi, N. Marooka, and I. Suemune, Appl. Phys. Lett. **74**, 1254 (1999).